International Journal of Basic Science and Technology
May, Volume 10, Number 2, Pages 171 - 183 http://www.ijbst.fuotuoke.edu.ng/ 171
https://doi.org/10.5555/OHIX7423 **ISSN 2488-8648**

Amelioration of Dyslipidaemia and Antioxidant Parameters in Alloxan-Induced Diabetic Rats Treated with a Hydrazone Derived from 4-Aminoantipyrine and Butanedione, and its Ni(II) Complex.

[*1] Agbo, N.J. and [2] Ukoha, P.O.

[1]Chemistry Advanced Research Centre, Sheda and Science and Technology Complex (SHESTCO), Garki-Abuja, Nigeria
[2]Coordination Chemistry and Inorganic Pharmaceuticals Unit, Department of Pure and Industrial Chemistry University of Nigeria, Nsukka, Enugu State, Nigeria

Article Information

Article # 10031
Received: 7th April. 2024
1st Revision: 2nd May. 2024
2nd Revision: 9th May 2024
Acceptance:11th May 2024
Available online:
124h May 2024.

Key Words
Alloxan, 4-aminoantipyrine, Butanedione, Diabetes, Dyslipidaemia, Hydrazone

Abstract

Investigating the antioxidant and antihyperlipidemic properties of c[Ni(HL)$_2$]Cl$_2$ was the goal of this work. Diabetic rats induced with alloxan. After two days of a single intraperitoneal injection of Alloxan (140 mg/kg), diabetes in albino rats was verified. Oral glibenclamide (200 mg/kg) and HL and [Ni(HL)$_2$]Cl$_2$ (200 and 400 mg/kg, respectively) were given every day for 14 days. Rats that had fasted overnight were killed on the fifteenth day, and blood was drawn to measure total cholesterol (TC), low density lipoprotein cholesterol (LDL), high density lipoprotein cholesterol (HDL), and total glycerides (TG). In order to assess the in vivo antioxidant activity of HL and [Ni(HL)$_2$]Cl$_2$, anti-oxidants were homogenised, and lipid peroxidation assays (Malondialdehyde (MDA), glutathione (GSH), catalase (CAT), erythrocyte superoxide (SOD), and glutathione peroxidase (GPx) were conducted in rats treated with HL and [Ni(HL)$_2$]Cl$_2$ and control groups. When compared to the diabetic control group, HL and [Ni(HL)$_2$]Cl$_2$ at doses of 200 and 400 mg/kg shown significant improvements in MDA, GSH, CAT, GPx, and SOD and significant reductions in blood glucose and lipid profiles. We determined that HL and [Ni(HL)$_2$]Cl$_2$ exhibit antihyperlipidemic and potentials on total glycerides (TG) and cholesterol (TC)

***Corresponding Author:** Agbo, N.J. agbo.ndj@gmail.com

Introduction

According to several studies (Farombi *et.al*, 2007; Solani, (2018); Alsaad *et.al*, 2007; Zadhoush *et al*, 2015; Milosevic *et. al*, 2019; Arkew *et al*., 2021) the rapid rise in diabetic complications is caused by abnormal values of some hypolipidemic and biochemical parameters as well as the toxic side effects of medications used to treat diabetes. As diabetic complications increase and free radicals are produced in the pathophysiology of the disease, this has led to abnormalities in biochemical and lipidemic indices (Soh Désiré, 2021; Oyedemi *et al*., 2011).

Serum lipid levels have been shown to rise with diabetes mellitus and are thought to be the main factor contributing to coronary heart disease in diabetics (Murugan *et al*, 2009). A weakness in antioxidant defence systems and an increase in the formation of oxygen-free radicals such superoxide, hydrogen peroxide (H_2O_2), and hydroxide (OH^-) radicals are the causes of increased oxidative stress in diabetes mellitus (Moussa, 2008). Lowering blood glucose levels, minimising the risk of the onset and progression of disease complications, particularly cardiovascular risk reductions, and correcting dyslipidemia are the three main objectives of research on treatment strategies for diabetes mellitus (Uhuo *et al*., 2022; Holman *et al*., 2008).

As to Holman *et al*. (2008), the current treatments for diabetes consist of insulin treatment, oral hypoglycemic medication, and lifestyle adjustment through diet and exercise. Additional approaches to managing diabetes mellitus include bariatric surgery (Robinson, 2009), islet cell transplantation (Lakey *et al*., 2003), and pancreatic transplantation (Larsen, 2011).

According to Stefano and Watanabe (2010), the majority of medications used in clinical practice have major side effects that include haematological consequences, hypoglycemia coma, and disruptions of the liver and kidney. This opens the door to the quest for drugs that have negligible or no side effects for the management of diabetes and its consequences. The purpose of this study was to examine the potential ameliorative effects of therapy with 200 and 400 mg/kg b.w. of HL and [Ni(HL)$_2$]Cl$_2$, respectively, on the antioxidant profile and lipid profile of rats with alloxan-induced diabetes after the glucose level was

https://doi.org/10.5555/OHIX7423 ISSN 2488-8648

lowered. Ultimately, this investigation demonstrated that, in comparison to diabetic rats not receiving treatment, HL and its Ni(II) complex restored the lipid profiles and antioxidant levels in alloxan-induced diabetic rats.

Materials and Methods

Chemicals/Compounds, synthesis of compounds

Zigma provided all of the chemicals, which were of the highest purity and quality suitable for use as analytical reagents. Unless otherwise specified, used as received. For the synthesis, a solvent that was readily available in the market was distilled.

The ligand 3-[2-hydrazinylidene-1,5-dimethyl-3-oxo-2-phenyl-2,3-dihydro-1H-pyrazol-4-yl] 1-phenylbutanedione, was prepared using Heinosuke's (1969) technique. A solution of sodium nitrite (0.0009 mol) was added to diluted hydrochloric acid (1 cm^3 in 5 cm^3) and 4-ammonioantipyrine (0.0006 mol) was stirred by hand at 5 °C to diazotize it. With mechanical stirring at room temperature, the resultant diazotized 4-aminoantipyrine was added to a solution containing 0.0305 mol of sodium acetate and 0.0006 mol of 1-phenyl-1,3-butanedione. The orange powder product (51.37, yield %, 66 M. Pt ^{0} C) was gathered and evaluated for HL. (scheme 1).

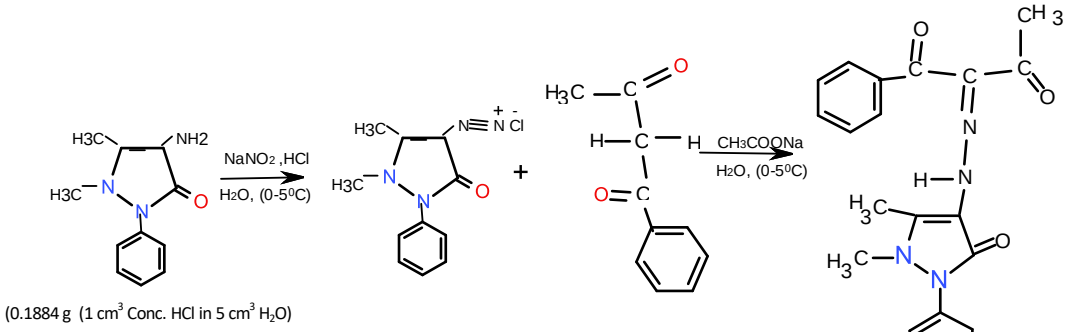

Scheme 1: synthesis of 3-[2-(1,5-dimethyl-3-oxo-2-phenyl-2,3-dihydro-1*H*-pyrazol-4-yl)hydrazinylidene]-1-phenylbutanedione HL

The *El-said et al.* (2001) approach was used to create the metal complexes. Two moles of a metal salt and one mole of 3-[(E)-(1,5-dimethyl-3-oxo-2-phenyl-2,3-dhydro-1H-Pyrazole-4-yl)diazenyl]-1-Phenylbutandione were combined to form the a solution which was agitated for six hours at 60 degrees Celsius in approximately 50 cm^3 of Ethanol. After filtering out the resultant solids formed, they were recrystallized in Ethanol and dried on $CaCl_2$.

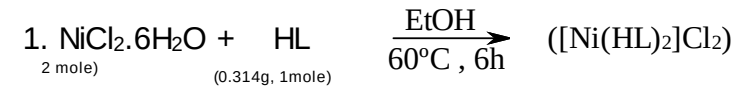

scheme 2: Reaction Equation

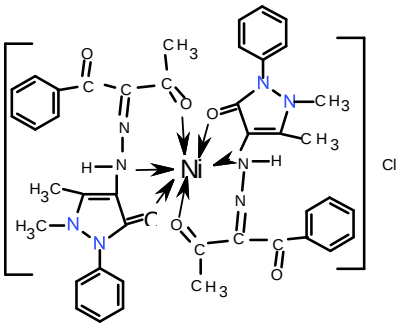

structure of $[Ni(HL)_2]Cl_2$

Experimental animals: The University of Nigeria, Nsukka, Faculty of Veterinary Medicine Institutional Animal Care and Use Committee (Ethical Approval Reference Number: FVM-UNN-IACUC-2023-11/132) was followed in all research involving albino rats and mice.

For experimental diabetes research, a total of 35 albino rats (average body weight: 120 ± 20 g) were employed, while 150 mice were used for toxicity tests (LD_{50}).

https://doi.org/10.5555/OHIX7423 ISSN 2488-8648

These were acquired from the University of Nigeria, Nsukka, Enugu State, Nigeria's Animal House, Faculty of Veterinary Medicine. Standard environmental conditions were maintained in the animal housing. For seven days, they were accustomed to the laboratory environment.

Experimental Design: The animal experiments adhered to the Guide for the Care and Use of Laboratory Animals. Animals were weighed and randomly assigned to seven groups and treated as follows:

Table 1: Animal groupings and administered samples

Rat groups	Number of rats	Treatment
Group A	5	Normal control (No diabetes + No Treatment)
Group B	5	Positive Control (Induced diabetes + No treatment
Group C	5	Standard Control (Induced diabetes + 200 mg/kg of b. w glibenclamide/standard drug treatment)
Group 1A	5	Induced diabetes + 200 mg /kg b. w of HL treatment
Group 1B	5	Induced diabetes + 400 mg /kg b. w of HL treatment
Group 2A	5	Induced diabetes + 200 mg /kg b. w of $[Ni(HL)_2]Cl_2$ treatment
Group 2B	5	Induced diabetes + 400 mg /kg b. w of $[Ni(HL)_2]Cl_2$ treatment

Diabetes Induction

Rats in groups 1 through 5 were intraperitoneally given 120 mg/kg body weight of alloxan monohydrate (dissolved in 0.9% sterile NaCl solution of pH 7) in order to induce diabetes; the rats' blood glucose levels had already been measured.

The animals' tail arteries were then used to draw blood, and Accu-check active glucometer—manufactured by Roche Diabetes Care, India - was used to measure the animals' blood glucose levels. For the purpose of the investigation, rats with serum glucose levels between 250 and 400 mg/dl that demonstrated distinct symptoms of polyuria, polyphagia, and polydipsia after a single day were classified as diabetics (Osinubi *et al*., 2006; Eyo *et al*., 2011). Throughout the course of the 14-day treatment and feeding period, the animals' blood glucose levels were checked on days 7 and 14.

Blood sample Collection: Rats were given a light chloroform anaesthesia, allowed to fast for the entire experiment, and then sacrificed by jugular vein incision. About five millilitres of blood was withdrawn from each rats, which was placed into a dry centrifuge tube and left to clot at room temperature (24–26°C). After that, the serum and clot were separated using centrifugation, which was done for 15 minutes at 1000–2000 revolutions per minute. Serum collected was stored in sterile bottles and kept at 4 °C

Cholesterol Determination: This was carried out using the methodology of Li-Hua Li *et al*. (2019). Ten microliter of blood sample, distilled water, standard reagent, and a labelled test, standard, and blank test tube were each filled with the appropriate contents. Next, each test tube was filled with 1000 µl of reagent R1, mixed, and allowed to incubate for 10 minutes at 37 ^{0}C. At 546 nm, the absorbance of each cuvette was measured and recorded. Using the following formula, the cholesterol concentration (mg/dl) was determined

$$Chol.Conc.(mg/dl) = \frac{Abs\ of\ sample}{Abs\ of\ standard} \times Conc.of\ standard\ \ldots\ldots..Eq\ 1$$

Serum Triglycerides (Tag) Determination

This was done according to Tietz (1976) method. The 5 µl of the distilled water was added into test tube blank, 5 µl of the standard reagent was added into another test tube and 5 µl of the sample was added into another test tube. Then, 500 µl reagent R_1 was added into each test tube and mixed. This was incubated for 5 min at 37 ^{0}C. The absorbance of all the cuvettes was read and recorded at 546 nm.

$$TAG(mmol/l = \frac{change\ in\ Abs.sample}{change\ in\ Abs\ standard} \times standard\ Conc.\ \ldots\ldots Eq\ 2$$

https://doi.org/10.5555/OHIX7423 ISSN 2488-8648

High Density Lipoprotiens (HDL) Determination
The concentration of cholesterol in high density lipoproteins (HDL) was measured using a Randox kit in accordance with Kazumi (2021) methodology. Following the pipetting of 100 µl of the serum and standard into the centrifuge tube, 500 µl of the diluted precipitation reagent (R1) was added right away. After mixing the contents and letting them stand at 25 ^{0}C for ten minutes, the mixture was centrifuged for fifteen minutes at 3500 rpm. Following centrifugation, the supernatant's cholesterol content was measured. 50 µl each of the sample supernatant, standard, and blank were put into three test tubes with the labels test, sample supernatant, standard, and blank. Next, the test tubes were filled with 500 µl of each Cholesterol reagent solution, mixed, and incubated for 10 minutes at 25 ^{0}C. In 60 minutes, read the absorbance at 500 nm.

$$HDL\ (mg/dl) = \frac{change\ in\ Abs\ \ sample}{change\ in\ Abs\ standard} \times Conc.of\ standard\ \ \ldots\ldots\ldots Eq\ 3$$

Low Density Lipoproteins (LDL) Determination
Method of Dieter *et al*. (2023) was applied. When polyvinyl sulphate (pvs) was used to precipitate the LDL fraction in the presence of polyethylene glycol monomethyl ether, the difference between the total cholesterol and the cholesterol content of the supernatant was used to calculate LDL-Cholesterol.
.

$$\text{LDL (mg/dl)} = \text{total cholesterol} - \text{TAG} - \frac{\text{HDL Cholesterol}}{5}\ \ldots\ldots\ldots Eq\ 4$$

Superoxidismutase (SOD) Assay: Superoxide dismutase activity was assayed by Jakub *et. al.* (2020) method. One (1 ml) of sodium phosphate buffer (pH 7.6) was added inside test tube. 100 µl of serum sample (blood) was added into test tube. Then, 75 µl of xanthine oxidase was added, mix and the initial absorbance was taken after 30 sec. The final absorbance was taken after 3 min at 480 nm. The changing rate of absorbance is used to determined superoxide dismutase activity.
.

Catalase Assay: The activity of catalase was assayed by Vetrano *et al*., (2005) method. 1 ml of phosphate buffer was pipette in the test tube. 1 ml of hydrogen peroxide (H_2O_2) was added. Then, 100 µl of serum samples were added and mix. The reaction was initiated by adding (2 ml of glacial acetic acid +1 ml of potassium dichromate reagent) 1 ml portion of this mixture. Absorbance of the reaction was taken in minute interval into 3 places at 420 nm

$$Catalase\ activity\ (U/ml) = 0.23 \times \frac{\log Abs\ 1}{Abs\frac{}{0.00693}}\ \ \ldots\ldots\ldots\ldots Eq\ 5$$

Gluthione Peroxidase Estimation: This was carried out using the Deshpande *et al*. (2018) approach. Serum samples with a known volume of 0.1 ml were pipetted into a test tube. The test tube was filled with 1 ml each of the diluted reagent (R1) and the diluting reagent (R2), after they had been mixed. After 30 seconds, the original absorbance was measured. After a minute, the final absorbance was measured at 340 nm. The following formula was used to compute glutathione peroxidase activity:

$$\textbf{Gluthione Perioxidase (in } U/L\ of\ haemolysate) = 8412 \times Abs\ at\ 340\frac{nm}{minute} \ldots Eq\ \ldots 6$$

Where U/L= Unit/ Liter

Glutathione Reduced
The Alisik *et al.*, (2019) method was used to measure the reduced glutathione concentration. 1.8 millilitres of EDTA solution were combined with 0.2 millilitres of the sample. 3.0 millilitres of precipitating reagent were added, well mixed, and allowed to stand for five minutes prior to centrifugation. A spectrophotometer was used to measure the colour generated at 412 nm

https://doi.org/10.5555/OHIX7423 ISSN 2488-8648

after adding 4 ml of 0.3 M disodium hydrogen phosphate solution and 1 ml of DTNB reagent to 2 ml of the supernatant. The same protocol was applied to a series of standard solutions containing 20–100 mg of reduced glutathione. For plasma, the data were given as mg/dl.

Malondialdehyde Estimation

As stated by Tang *et al.* (2019), the amount of malondialdehyde (MDA), the lipid peroxidation product, was measured spectrophotometerically in order to assess lipid peroxidation. In a test tube, 0.1 ml of the serum and 0.9 ml of distilled water were combined. Additionally, the mixture was supplemented with 0.5 ml of 25% TCA (trichloroacetic acid) and 0.5 ml of 1% TBA (thiobarbituric acid) in 0.3% NaOH. After 40 minutes of boiling in a water bath, the mixture was chilled in cold water. After the solution had cooled, 0.1 millilitre of 20% sodium dodecyl sulphate (SDS) was added and thoroughly mixed. In comparison to a blank, the absorbance was measured at wavelengths of 532 nm and 600 nm.

$$Malondiadehyde\ (MDA) = \frac{Abs\ A - Abs\ B}{0.5271} \times 10 \quad \ldots\ldots\ldots Eq\ 7$$

Where, Abs A= absorbance at 532 nm, Abs B= absorbance at 600 nm, 10= dilution factor,

Statistical analyses: Data from the lipid profile and serum electrolytes studies were analysed using one-way analysis of variance (one-way ANOVA), and service solutions (SPSS) version 20. Results were expressed as mean ± SD. Values with different superscripts are considered significant at $p < 0.05$.

Results

Interpretation of the chemical structure

The synthesis and characterization of this ligand HL and its Ni(II) complex have been reported (Agbo and Ukoka, 2023).

Attempts have been made to propose the structures of the complex and the ligand HL using spectroscopic methods such as elemental data analysis and NMR, IR, UV, and mass spectra. Despite multiple tries, the HL and metal complex single crystals could not be obtained.

This particular absorption peak in the $[Ni(HL)_2]Cl_2$ complex spectra was seen to shift to a higher position after HL complexed. This was consistent with other azopyrazolones complex discoveries made before (El. Saied *et al*., 2001). Some of the peaks in the complexes' spectra that were seen for the (C=O) stretch in HL moved to different frequencies in some of the complexes, indicating that C=O carbonyl was involved in the complexation.

Peak of the $[Ni(HL)_2]Cl_2$ complex at 553.59 cm^{-1}

In the ultraviolet $[Ni(HL)_2]Cl_2$, the Cl_2 spectrum displays a single, strong absorption band at 737.5 nm (13557 cm^{-1}). When $[Ni(HL)_2]Cl_2$ complexes were compared to $CuSO_4$ and NaCl salts (Tharmaraj *et al.*, 2009), it was found that the complexes had Cl^- inside co-ordination spheres with metal ions, indicating that $[Ni(HL)_2]Cl_2$ was electrolyte.

^1H NMR of HL was conducted using $CDCl_3 + CD_3OD$ solvents which indicates that it existed in hydrazo form (Imran Ali *et al.* (2013). HL exhibits peaks at 1.88, 1.99 & 2.16 ppm (3H,s), and 3.28 (3H,s), denoting, respectively, the methyl protons of the pyrazolone ring, $C\text{-}CH_3$, and $N\text{-}CH_3$. Another peak

An (N-H) stretching vibration was indicated by a broad peak in the IR spectra of HL at 3415 cm^{-1} (Altaf *et al*., 2023). El-Saied et al. (1993) identified the carbonyl (C=O) group of pyrazolone as the source of the peak at 1661 and 1643 cm^{-1}, while the C=O of diketones was responsible for the peaks around 1810 and 1750 cm^{-1}. The (C=N) stretching vibration was attributed to a sharp peak at 1597cm^{-1}.

suggested M-O vibration. M-Cl vibrations were responsible for the other peak at 457.14 cm^{-1} in the $[Ni(HL)_2]Cl_2$ spectrum (Ajayeoba *et al*., 2017).

When the electronic spectra of HL and its complex in methanol (10^{-4} M) were compared, they revealed a great deal of similarity in terms of band location and intensity. There were two absorption bands visible: 413 and 522 nm. The bands were ascribed to the conjugated bonds' $\pi \rightarrow \pi^*$ transitions and the ligand's non-bonding electrons' $n \rightarrow \pi^*$ transitions.

around 4.88(1H, s) and 6.35(1H, s) indicates the N-H proton and solvent (HDO) peak. Phenyl protons were responsible for peaks at 7.44 and 7.845(1H, d), 7.50 and 7.52(1H, s).

The HL ^{13}C NMR spectrum revealed fourteen (14) peaks, each of which represents the number of carbon atoms in the hydrazo structure. The carbon atoms of the carbonyl groups were represented by the peaks at 197.22 and 194.16 ppm. The carbon atoms of the C=O methyl and C=N groups were shown to be responsible for the peaks at 182.78 ppm and 178.36 ppm, respectively. The aromatic rings substituent's carbon atom peaks were found at 133.4767 ppm, 47.655 ppm,

https://doi.org/10.5555/OHIX7423 ISSN 2488-8648

34.01 ppm, and 29.44 ppm. The antipyrine ring's carbon atom peaks emerged at ppm 128.88, 126.25, Mass spectrometer readings revealed signals at m/z 464.5385, m/z 384.336 (indicating that dibenzoyl methane ($–C_6H_5$) was removed from the ligand), and m/z 306.4805 (indicating fragmentation at the second Based on the available information, it was evident that the ligand functioned as a tridentate and coordinated via the carbonyl group's nitrogen and oxygen to form

Biological Investigation of -[2-(1,5-dimethyl-3-oxo-2-phenyl-2,3-dihydro-1H-pyrazol-4-yl)hydraziny -lidene]-1-phenylbutanedione and its Complexes on Diabetic Rats

HL and $[Ni(HL)_2]Cl_2$ treatments of diabetic rats demonstrated the compounds' advantageous effects on reversing the lipid metabolism imbalance associated with diabetes. Thus, our investigation suggests that even at low and higher dosages of the compounds, HL and $[Ni(HL)_2]Cl_2$ increased the serum lipids and antioxidant levels in blood against damage due to diabetes.

and 96.21. The methyl rings' carbon atoms gave rise to peaks at 24.41, 22.45, and 9.67 ppm, respectively.
benzoyl group). A fragment in the mass spectrum with a m/z value of 922.872 indicates that the ligand is likely present in a dimeric form through H-bonding.

hydrogen bonds, substituting metal ions for the H in certain complexes. They ascribed the Ni (II) complex of HL an octahedral geometry.
Effects of Treatment with Low and High dose of HL and $[Ni(HL)_2]Cl_2$ on Blood Glucose Concentrations.
Table 2 displays the blood glucose concentrations that were measured. When compared to the final concentrations recorded in the control group, blood glucose levels in the diabetes treatment groups reduced significantly ($p < 0.05$). When compared to the untreated diabetic rats in group B, the blood glucose concentration of the diabetic group treated with low dose HL fell significantly ($p < 0.05$) on the 7th and 14th day. Compared to the diabetic group treated with glibenclamide, the diabetic group receiving high dose HL experienced a significant ($p < 0.05$) decrease in blood glucose concentration.

Table 2: Effect of the Synthesized Samples on the Blood Glucose Concentration of Experimental Diabetic Rats

Group	Before Induction (mg/dL)	After Induction (mg/dL)	After 7 Days Treatment (mg/dL)	After 14 Days Treatment (mg/dL)
A	71.60±6.84	72.40±7.57	74.00±12.85	74.40±7.23
B	73.40±9.91	308.00±65.36	414.00±45.67	527.80±37.12
C	76.40±5.32	294.60±77.75	175.00±60.38	116.20±18.23
1A	73.40±9.48	360.40±126.40	195.40±58.99	101.20±19.41
1B	79.20±11.23	274.40±49.71	149.60±41.82	103.60±8.38
2A	80.00±7.31	322.80±95.71	145.40±48.64	92.20±23.44
2B	79.60±11.01	353.60±85.82	109.60±21.29	88.40±9.21

Legend: A= Normal control (No diabetes + No Treatment), B= Positive Control (Induced diabetes + No treatment), C= Standard Control (Induced diabetes + 200 mg/kg of b. w glibenclamide/standard drug treatment), 1A= Induced diabetes + 200 mg /kg b. w of HL treatment, 1B= Induced diabetes + 400 mg /kg b. w of HL treatment, 2A= Induced diabetes + 200 mg /kg b. w of $[Ni(HL)_2]Cl_2$ treatment and 2B= Induced diabetes + 400 mg /kg b. w of $[Ni(HL)_2]Cl_2$ treatment

Effect of the HL and $[Ni(HL)_2]Cl_2$ on hyperlipidaemia of Experimental Rats

By measuring the serum levels of TC, TG, LDL-C, and HDL-C, the lipid profile was ascertained (Table 3). After two weeks of the trial, the levels of TC total

cholesterol, LDL cholesterol, LDL cholesterol, and TAG triacylglycerols were significantly higher in the untreated diabetic rats than in the normal animals. Glibenclamide treatment produced TG (1.07±0.05) and HDL (1.17±0.09) concentrations that were non-significantly ($p > 0.05$) lower than those of the normal

https://doi.org/10.5555/OHIX7423 ISSN 2488-8648

control group A (1.13±0.11) and (1.22±0.07), respectively. Additionally, glibenclamide treatment—a typical medication—brought the rats' total cholesterol and LDL down to almost normal levels when compared to normal control rats. Treatment with HL and $[Ni(HL)_2]Cl_2$ at low and high doses showed an anti-lipidaemic effect and improved the serum lipid profile significantly ($P < 0.05$).

Table 3: HL and $[Ni(HL)_2]Cl_2$ effect on the Lipids profile of Experimental Rats

Groups	TAG(mmol/L)	Total Cholesterol	HDL	LDL
A	1.13±0.11	2.61±0.26	1.22±0.07	1.12±0.33
B	1.98±0.19	3.82±0.14	1.69±0.29	1.74±0.16
C	1.07±0.05	2.64±0.15	1.17±0.09	1.25±0.12
1A	1.06±0.08	2.74±0.15[d]	1.22±0.09	1.24±0.12
1B	1.13±0.12	2.57±0.08	1.22±0.09	1.15±0.10
2A	1.08±0.07	2.56±0.15	1.22±0.07	1.14±0.11
2B	1.05±0.03	2.53±0.13	1.21±0.09	1.11±0.10

Legend: A= Normal control (No diabetes + No Treatment), B= Positive Control (Induced diabetes + No treatment), C= Standard Control (Induced diabetes + 200 mg/kg of b. w glibenclamide/standard drug treatment), 1A= Induced diabetes + 200 mg /kg b. w of HL treatment, 1B= Induced diabetes + 400 mg /kg b. w of HL treatment, 2A= Induced diabetes + 200 mg /kg b. w of $[Ni(HL)_2]Cl_2$ treatment and 2B= Induced diabetes + 400 mg /kg b. w of $[Ni(HL)_2]Cl_2$ treatment

HL and $[Ni(HL)_2]Cl_2$ effect on the antioxidant Concentration of Experimental Rats

Table 4 listed the amounts of reduced gluthione (GSH) and malondialdehyde (MDA) as well as the activities of superoxide dismutase (SOD), gluthione peroxidase (GPX), and catalase (CAT) in the experimental rats. When compared to the diabetic group treated with glibenclamide, the activity of SOD in the group given both low and high dosages of HL was higher ($p < 0.05$). CAT activity rose significantly ($p < 0.05$) in the diabetic group treated with low and high dosages of HL or $[Ni(HL)_2]Cl_2$ compared to the untreated diabetic group B. Compared to the control group, the diabetic group receiving both low and high dosages of HL or $[Ni(HL)_2]Cl_2$ experienced a significant ($p < 0.05$) drop in GPx activity. The GSH concentration of diabetic untreated rats in group B (3.41±0.52) was found to be significantly higher ($p < 0.05$) than that of the normal control group A (2.49±0.28). GSH concentrations were non-significantly ($p > 0.05$) greater after treatment with glibenclamide (standard medication) than in normal control group A (2.49±0.28). When compared to the diabetic group treated with glibenclamide (group C), the activity of MDA in the diabetic group receiving low and high dosages of HL or $[Ni(HL)_2]Cl_2$ was reduced ($p < 0.05$). In comparison to the normal control group A (1.49±0.28), Table 4 demonstrates a significant ($p < 0.05$) increase in the MDA activities of group B (2.24±0.34) diabetic untreated rats.

Table 4: HL and $[Ni(HL)_2]Cl_2$ effect on the antioxidant Concentration of Experimental Rats

Grp	GSH	SOD	GPx	CAT	MDA
A	2.49±0.28	11.09±0.18	10.76±1.12	1.14±0.06	1.49±0.28
B	1.41±0.52	10.46±0.01	12.76±2.06	0.38±0.47	2.24±0.34
C	2.58±0.24	11.24±0.21	10.51±1.42	1.25±0.04	1.29±0.21
1A	2.53±0.09	11.35±0.09	10.86±0.48	1.15±0.08	1.22±0.07
1B	2.55±0.09	11.30±0.13	10.34±0.71	1.11±0.05	1.14±0.08
2A	2.60±0.10	11.28±0.18	10.00±1.57	1.11±0.05[ab]	1.13±0.11
2B	2.42±0.11	11.27±020	9.82±0.47	1.07±0.04	1.12±0.08

Legend: A= Normal control (No diabetes + No Treatment), B= Positive Control (Induced diabetes + No treatment), C= Standard Control (Induced diabetes + 200 mg/kg of b. w glibenclamide/standard drug treatment), 1A= Induced diabetes + 200 mg /kg b. w of HL treatment, 1B= Induced diabetes + 400 mg /kg b. w of HL treatment, 2A= Induced diabetes + 200 mg /kg b. w of $[Ni(HL)_2]Cl_2$ treatment and 2B= Induced diabetes + 400 mg /kg b. w of $[Ni(HL)_2]Cl_2$ treatment

https://doi.org/10.5555/OHIX7423 ISSN 2488-8648

Discussion

Hyperlipidemia, or abnormally high levels of cholesterol, triglycerides, and lipoproteins, is linked to diabetes. Since insulin has an anti-lipolytic action by blocking hormone-sensitive lipase, the aberrant rise in serum lipid levels in the animals in the diabetic control group is mostly caused by an enhanced mobilisation of free fatty acids and peripheral fat deposits (Renganathan *et.al*, 2020). By increasing the production of insulin or imitating its action, the administration of high and low doses of HL and $[Ni(HL)_2]Cl_2$, respectively, would have altered the lipid profile of diabetic individuals. Consequently, elevated insulin secretion promotes the manufacture of fatty acids and their integration into the triglycerides found in both adipose and hepatic tissue (Madić *et al*. 2021).

The rate of diffusion across the intestinal mucosa was similarly slowed down by the high and low doses of HL and $[Ni(HL)_2]Cl_2$, respectively, which decreased the absorption of triglycerides and cholesterol (Hassan *et al*. 2022). Furthermore, carbonyl compounds have been shown to have lipid-lowering effect by several scientists (Hassan *et al*. 2022). The combined effect of these chemical compound types present in the samples would explain the observed hypolipidemia.

The amount of oxidative stress can be determined by measuring MDA, the end product of lipid peroxidation Tang *et al.* (2019). In fact, the decrease in lipid peroxidation brought on by the increased synthesis of antioxidant enzymes explains the reduction in MDA. In the current study, the MDA level in diabetic participants was lower in the HL and $[Ni(HL)_2]Cl_2$ (20 and 500 mg/kg), respectively, compared to the untreated group. Because of their capacity to prevent lipid peroxidation, HL and ($[Ni(HL)_2]Cl_2$) fortify the antioxidant defence system. As seen in the untreated diabetic group B, induced hyperlipidemia causes an increase in oxygen free radical generation, which in turn causes lipid peroxidation (Murtaza *et al*., 2021).

The enzyme superoxide dismutase (SOD) disproportionates endogenous harmful superoxide radicals into hydrogen peroxide (H_2O_2), which has a significant impact on the biological defence system (Ikewuchi *et al*. 2017). The SOD activity in the diabetic control lot rats in this study declined. In contrast, compared to the untreated diabetic group B, the reference product and the doses of 200 and 400 mg/kg of HL and $[Ni(HL)_2]Cl_2$ increased the amount of SOD activity in the liver. Thus, HL and $[Ni(HL)_2]Cl_2$ had a major impact on the body's oxidative defence system.

The tetrameric enzyme catalase (CAT) effectively transforms H_2O_2 into oxygen and water. Unlike glutathione, catalase's affinity for hydrogen peroxide increases only in the presence of elevated H_2O_2 levels (Chelikani *et.al*, 2004) CAT, which is widely distributed in oxygen-dependent organisms, shields cells from reactive oxygen species (ROS)-induced oxidative damage (Ighodaro, 2018). Accordingly, the current study's observation of increased catalase activity with HL and $[Ni(HL)_2]Cl_2$ would indicate a drop in the cell's ROS level.

Glutathione (GSH) participates in numerous biological processes and functions as an intra- and extracellular antioxidant. Lipid peroxidation levels are lowered as a result of the reduction of hydrogen peroxide (Miaffo, 2019). Furthermore, GSH is essential for cells' defence against oxidative species such as free oxygen radicals (Arivazhagan *et.al*, 2001) Hepatic GSH levels rose in this study across all chemical dosages. This rise would be expected given the chemicals' powerful ability to protect cells from reactive oxygen species and free radicals.

References

Agbo, N.J and Ukoha, P.O. (2023). Structure and Antimicrobial studies of New Hydrazone ligand, 3-[2-hydrazinylidene-1,5-dimethyl-3-oxo-2-phenyl-2,3-dihydro-1H-pyrazol-4-yl] 1-phenylbutanedione and its Co(II), Fe(III),Ni(II) and Cu(II) Complexes. Nigerian Research of Chemical Sciences 11(2),217-233.

Alsaad, K. O. and Herzenberg, A. M. (2007). Distinguishing diabetic nephropathy from other causes of glomerulosclerosis: an update. Journal of Clinical Pathology, 60(1): 18 – 26.

Arivazhagan, S., Balasenthil, S. and Nagini, S. (2000). Garlic and neem leaf extracts enhance hepatic glutathione and glutathione dependent enzymes during N-methyl-Nnitrosoguanidine (MNNG)-induced gastric carcinogenesis. Phytother Res.14(4):291–3.

Arkew, M., Yemane, T., Mengistu, Y., Gemechu, K. and Tesfaye, G. (2021). Hematological parameters of type 2 diabetic adult patients at Debre Berhan Referral Hospital, Northeast Ethiopia: a comparative cross-sectional study. PLoS One, 16(6): e0253286. https://dx.doi.or g/10.1371%2Fjournal.pone.0253286

Beverly, J. K. and Budoff, M. J. (2020). Atherosclerosis: pathophysiology of insulin resistance, hyperglycemia, hyperlipidemia, and inflammation. Journal. Diabetes. 12 (2):102–104. doi:10.1111/1753-0407.12970.

Chelikani, P., Fita, I. and Loewen, P. C. (2004). Diversity of structure and properties among catalases. Cell Mol Life Sci. 61(2):192–208.

Dieter, L., Hans-Ulrich, K and Frans, S. (2023). Measurement of Serum Low Density Lipoprotein Cholesterol and Triglyceride-Rich Remnant Cholester -ol as Independent Predictors of Atherosclerotic Cardiovascular Disease: Possibilities and Limitations. *Nutrients 15*(9), 2202; https://doi.org/10.3390/nu15092202

Deshpande, K. C., Kulkarni, M. M. and Rajput, D. V. (2018). Evaluation of glutathione peroxidase in the blood and tumor tissue of oral squamous cell carcinoma patients. *J Oral Maxillofac Pathol*. 22(3):447. doi: 10.4103/jomfp.JOMFP_140_17.

Distefano, J. K. and Watanabe, R. M. (2010). Pharmacogenetics of anti-diabetes *drugs. Pharmaceuticals*, 3:2610–46 [Crossref], [Google Scholar]

El.Saied, F. A., Ayad, M. I., Issa, R. M. and Aly, S.A.(2001). Synthesis and charactersation of Iron (III),Cobalt (II),Nickel(II) and copper(II) Complexes of 4-formylazoanilne Antipyrine. *Polish. J .Chem,* 75, pp 774.

Alisik, M., Neselioglu, S. and Erel, O. (2019). A colorimetric method to measure oxidized, reduced and total glutathione levels in erythrocytes. *Journal of Laboratory Medicine*, *43*(5), 269-277. https://doi.org/10.1515/labmed-2019-0098

Eyo, J. E., Ozougwu, J. C. and Echi, P. C. (2011). Hypoglycaemic effects of Allium cepa, allium sativum and zingiber officinale aqueous extracts on alloxan-induced diabetic rattus novergicus, *Medical Journal of Islamic World Academy of Sciences,* 19(3), pp.121-126.

Farombi, E. O. and Ige, O. O. (2007). Hypolipidemic and antioxidant effects of ethanolic extract from dried calyx of Hibiscus sabdariffa in alloxan-induced diabetic rats. Fundam Clin Pharmacol. 21(6),601-9. doi: 10.1111/j.1472-8206.2007.00525.x. PMID: 18034661.

Habib, M. Y., Islam, M. S., Awal, M. A. and Khan. M. A. (2005). Herbal products: A novel approach for diabetic patients. Pakistan Journal of Nutrition. 4(1), pp.17-21.

Habig, W. H., Pabst, M. J. and Jakoby, W. B. (1974). Glutathione s-transferase: The first enzymatic step in mercapturic acid formation. *The Journal of Biological Chemistry*, 24(22): 7130-7139.

Heinosuke, Y. (1967). Infrared Analysis of 2-pyrazolin-5-one Derivatives. Applied Spectroscopy. 23, pp.1969.

Holman, R. R., Paul, S. K. and Bethel, M. A. (2008). 10 Year follow-up of intensive glucose control in Type 2 diabetes. New Engl. J. Med. 359, pp 1577–89

Hussain, Z., Khan, J. A., Arshad, M. I., Muhammad, F and Abbas, R. Z. (2021). Protective effects of cinnamon, cinnamaldehyde and kaempferol against Acetaminophen-induced acute liver injury and apoptosis in mouse model. Pakistan Veterinary Journal. 41:25–32. doi:10.29261/pakvetj/2020.090.

Jakub, D., Małgorzata, S. D., Ewa, K., Małgorzata, K., Anna, D., Bartłomiej, D. and Małgorzata, P. (2020). Glutathione peroxidase (GPx) and superoxide dismutase (SOD) activity in patients with diabetes mellitus type 2 infected with Epstein-Barr virus. *PLoS One*. 15(3): e0230374.doi: 10.1371/journal.pone.0230374

Kazumi, M., Hiroyuki, S., Kensaku, A. , Takako, T., Yuki, K., Yoichi, I., Mitsuru, I., Tetsumi, I., Takeshi, M., Eiichi, A., Mizuki, S., Yuki, K. and Norihiko, K. (2021). A homogeneous assay to determine high-density lipoprotein subclass cholesterol in serum, Anal Biochem..15:613:114019. doi: 10.1016/j.ab.2020.114019.

Khurshid, A.H.M., Sharmin, R., Maruf, I., Hasibul, H. J., Mohiuddin, A. and Golam, M. (2018). Antidiabetic and hepatoprotective activities of *Bombax ceiba* young roots in alloxan-induced diabetic mice. J Nutr Health Food Sci. 6(5):1–7.

Lakey, J., Burridge, P. and Shapiro, A. (2003). Technical aspect of islet preparation and transplantation. Transp. Int. 16:613–32

Larsen, J.L. (2011). Pancreas transplantation: Indications and consequences. Available from: edrv. endjounals.org [last accessed 2 Feb 2013] [Google Scholar]

Lenzen, S. (2008). The mechanisms of alloxan and streptozotocin induced diabetes. *Diabetological*. 51, pp. 216 -226.

Li-Hua Li, Ewelina, P. D., Ying-Chen, H., Hsin-Bai, Z. and Cheng-Chih, H. (2019). Analytical methods for cholesterol quantification, Journal of Food and Drug Analysis,Volume 27(2),375-386, https://doi.org/10.1016/j.jfda.2018.09.001.

Madić, V., Petrović, A., Jušković, M., Jugović, D., Djordjević, L., Stojanović, G. and Vasiljević, P. 2021. Polyherbal mixture ameliorates hyperglycemia, hyperlipidemia and histopathological changes of pancreas, kidney and liver in a rat model of type 1 diabetes. *J Ethnopharmacol*. 265:113210. doi:10.1016/j.jep.2020.113210.

Miaffo, D., Guessom K.O. and Ledang T, N. (2019). Antidiabetic and antioxidant potentials of *Vitellaria paradoxa* barks in alloxan-induced diabetic rats. *Clin Phytosci* 5, 44. https://doi.org/10.1186/s40816-019-0141-z

Milosevic, D. and Panin, V. L. (2019). Relationship between hematological parameters and glycemic control in type 2 diabetes mellitus patients. Journal of Medical Biochemistry, 38(2): 164 – 171.

Moussa, S. A. (2008). Oxidative stress in diabetes mellitus. Roman J Biophys. 18:225–36 [Google Scholar]

Murugan, M, Uma, C. and Reddy, M. (2009). Hypoglycaemic and hypolipidemic activity of leaves of Mucuna pruriens in alloxan-induced diabetic rats. J Pharm Sci Technol 1:69–73 [Google Scholar]

Murtaza, S., Khan, J.A., Aslam, B. and Faisal, M. N. (2021). Pomegranate peel extract and quercetin possess antioxidant and hepatoprotective activity against Concanavalin A-induced liver injury in mice. Pak Vet J. 41:197–202. doi:10.29261/pakvetj/2020.097.

Nafisa, P. C., Chakradnar, V. L., Vandana, S. P. and Suresh, R. N. (2007), "An experimental evaluation of the antidiabetic and antilipidaemic properties of a standardized Momordica charantia fruit extract", *BMC Complementary and Alternative Medicine*, 7, pp. 29–55.

Nanu, R., Chitme, R. I. and Chanda, R. (2008). Antidiabetic activity of Nyctanthes arbortriris. Pharmacog Mag 4:16–21 [Web of Science ®], [Google Scholar]

Osinubi, A. A., Ajayi, O. G. and Adesiyun, A. E. (2006). Evaluation of the anti-diabetic effect of aqueous leaf extracts of Tripinanthus butungil in male spragne Dawley rats. *Medical Journal of Islamic World Academy of Science.* 16(1), pp. 41–47.

Oyedemi, S. O., Adewusi, E. A., Aiyegoro, O. A. and Akinpelu, D. A. (2011). Antidiabetic and haematological effect of aqueous extract of stem bark of Afzelia africana (Smith) on streptozotocin–induced diabetic Wistar rats. Asian Pacific Journal of Tropical Biomedicine, 1(5): 353 – 358.

Renganathan, S. and Pillai, R.G. (2020). Antioxidant activities of Dhanwantaram Kashayam–an Ayurvedic poly herbal formulation alleviates diabetic complications in rats. J Diab Metabol Disord. 19:1345–1355. doi:10.1007/s40200-020-00655-5.

Robinson, M.K. (2009). Surgical treatment of obesity: Weighing the facts. New Engl J Med 361:520–1 [Crossref] [PubMed] [Web of Science ®], [Google Scholar]

Solani D.M. (2018). Biochemical changes in diabetic retinopathy triggered by hyperglycaemia: a review, *African Vision and Eye Health* Vol. 77, No. 1. https://hdl.handle.net/10520/EJC-e827b5951

Soh, D., Nkwengoua, E., Tchebemou, B. B., Sidjui, S. L., Dzo, D. U., Mehreen, L., Bernd, S., Muhammad, S. A. and Nyassé, B. (2021). A new dammarane type triterpene glucoside from the aerial parts of Gouania longipetala (Rhamnaceae). *Natural Product Research.* 35:19, pages 3192-3203

Tang Q, Su Y. W. and Xian C. J. (2019). Determining Oxidative Damage by Lipid Peroxidation Assay in Rat Serum. Bio Protoc. 9(12):e3263. doi: 10.21769/BioProtoc.3263.

Tietz, N.W., Pruden, E. L. and Siggaard-Andersen, O. (1976). Electrolytes, blood gases and Acid-base balance. Pp 1188.

Uhuo, E.N., Godwin, K. O., Alaebo, P. O. and Ezeh, H. C. (2022). Haematological and Biochemical Parameters Assessment of Alloxan-Induced Diabetic Rats Treated with Ethanol Leaf Extracts of Adansonia Digitata (Baobab) Leaf. *Animal Research International* 19(2): 4469 – 4477

Vetrano, A. M., Heck, D. E., Mariano, T. M., Mishin, V., Laskin, D. L and Laskin, J. D. (2005). Characterization of the oxidase activity in mammalian catalase. *Journal of Biological Chemistry*, *280*(42), 35372-35381.

International Journal of Basic Science and Technology
May, Volume 10, Number 2, Pages 171 - 183 http://www.ijbst.fuotuoke.edu.ng/ 181
https://doi.org/10.5555/OHIX7423 **ISSN 2488-8648**

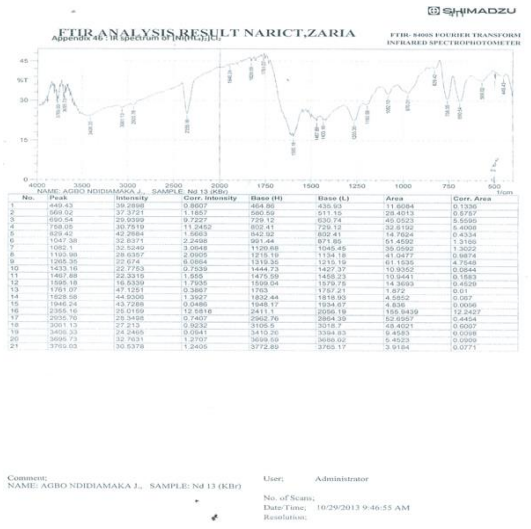

Fig 1: The IR Spectra of $[Ni(HL)_2]Cl$

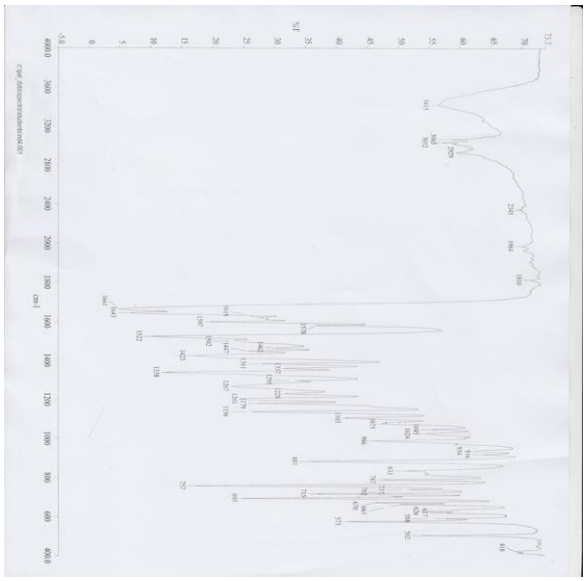

Fig 2: The IR spectra of HL

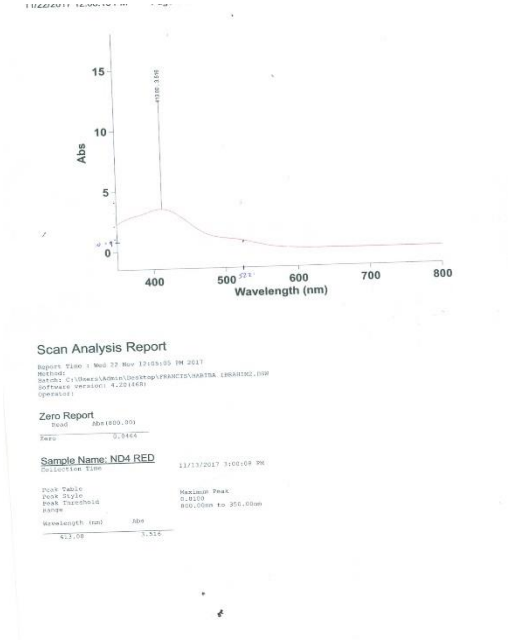

Fig 3: The Electronic Absorption spectrum of HL

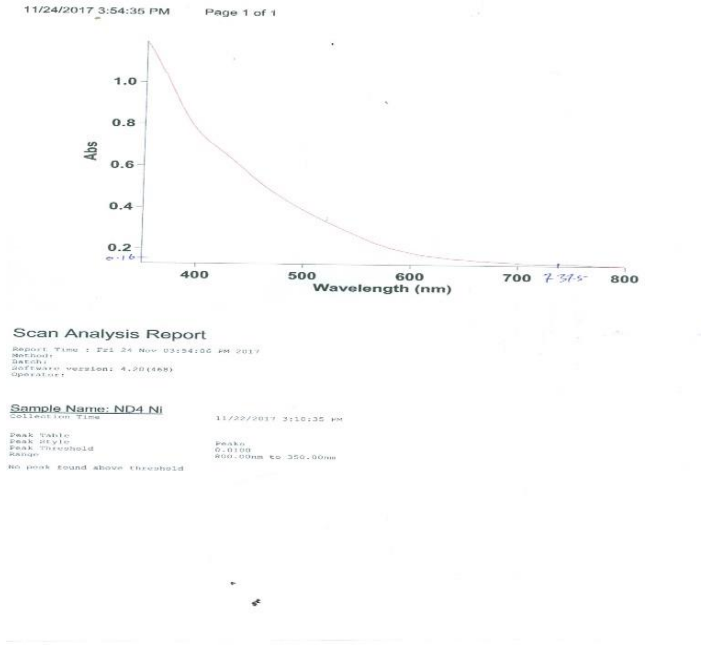

Fig 4: The Electronic Absorption spectrum of HL of $[Ni(HL^4)_2]Cl_2$

https://doi.org/10.5555/OHIX7423 ISSN 2488-8648

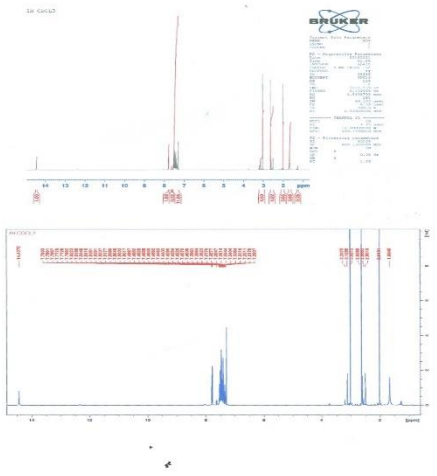

Fig 5: The ^{1}H NMR spectral of HL

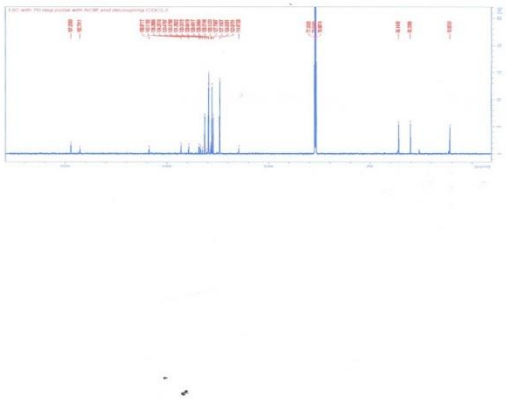

Fig 6: The ^{13}C NMR of HL

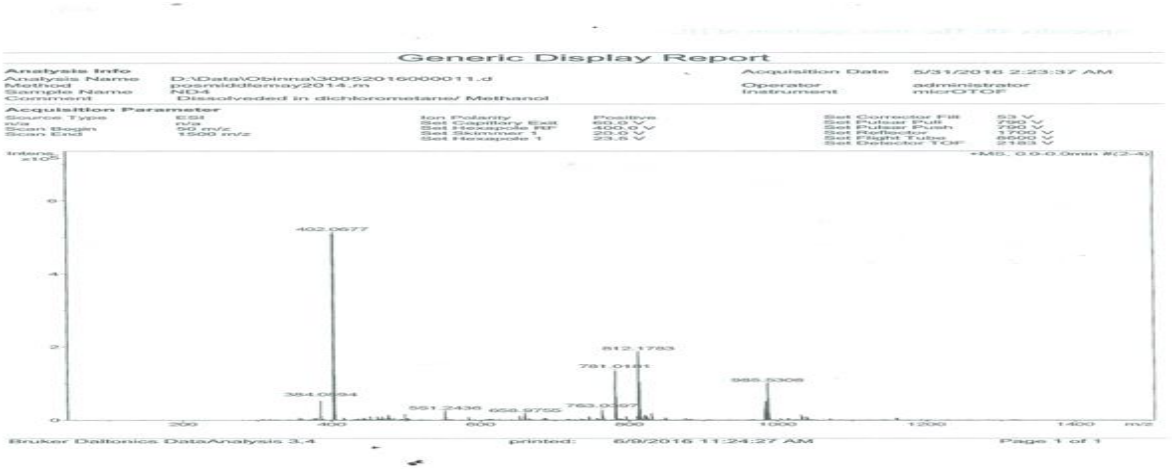

Fig. 7: The mass spectral of HL

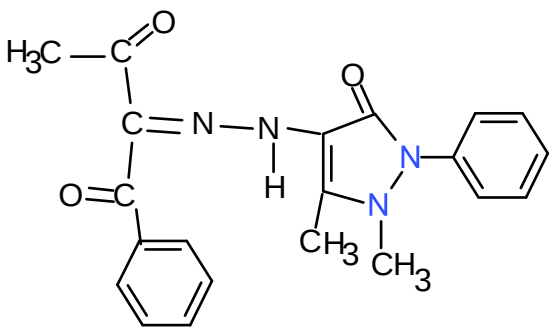

https://doi.org/10.5555/OHIX7423 ISSN 2488-8648

Fig 8: the structure of 3-[2-hydrazinylidene-1,5-dimethyl-3-oxo-2-phenyl-2,3-dihydro-1H-pyrazol-4-yl] 1-phenylbutanedione(HL)

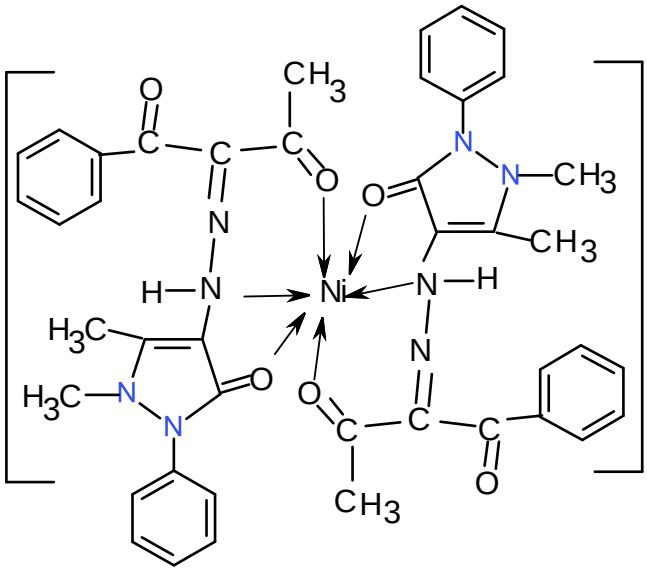

Fig 9: The structure of $[Ni(HL)_2]Cl_2$